## 1 Aging decreases osteocyte lacunar canalicular turnover in female C57BL/6JN mice

- 3 Ghazal Vahidi<sup>a</sup>, Connor Boone<sup>a</sup>, Fawn Hoffman<sup>b</sup>, & Chelsea Heveran<sup>a†</sup>
- 4 aDepartment of Mechanical & Industrial Engineering, Montana State University, Bozeman, MT, USA
- 5 bDepartment of Biomedical Sciences, College of Idaho, Caldwell, ID, USA
- 6 †Corresponding Author, T +1 406-994-2010, E chelsea.heveran@montana.edu,
- 7 https://orcid.org/0000-0002-1406-7439

2

#### **Abstract**

8

28

29

9 Osteocytes engage in bone resorption and mineralization surrounding their expansive lacunar-canalicular 10 system (LCS) through peri-LCS turnover. However, fundamental questions persist about where, when, 11 and how often osteocytes engage in peri-LCS turnover and how these processes change with aging. 12 Furthermore, whether peri-LCS turnover depends on tissue strain remains unexplored. To address these 13 questions, we utilized confocal scanning microscopy, immunohistochemistry, and scanning electron 14 microscopy to characterize osteocyte peri-LCS turnover in the cortical (mid-diaphysis) and cancellous 15 (metaphysis) femurs from young adult (5 mo) and early-old-age (22 mo) female C57BL/6JN mice. LCS 16 bone mineralization was measured by the presence of perilacunar fluorochrome labels. LCS bone resorption was measured by immunohistochemical marker of bone resorption. The dynamics of peri-LCS 17 18 turnover were estimated from serial fluorochrome labeling, where each mouse was administered two 19 labels between 2 and 16 days before euthanasia. Osteocyte participation in mineralizing their 20 surroundings is highly abundant in both cortical and cancellous bone of young adult mice but 21 significantly decreases with aging. LCS bone resorption also decreases with aging. Aging has a greater 22 impact on peri-LCS turnover dynamics in cancellous bone than in cortical bone. Lacunae with recent peri-23 LCS turnover are larger in both age groups. Our data support the hypothesis that peri-LCS turnover is 24 associated with cortical and intracortical positions for 22 mo mice but not for 5 mo mice. The impact of 25 aging on decreasing peri-LCS turnover may have significant implications for bone quality and 26 mechanosensation. 27

**Keywords:** Aging, osteocyte, lacunar-canalicular turnover, tissue strain

#### 1.0 Introduction

30

31

32

3334

35

36

37

38 39

40 41

42

43

44

4546

47

48

4950

51

52

53

54 55

5657

58

59

60

6162

The loss of bone fracture resistance in aging is a major public health problem<sup>1</sup>. Osteocytes, the most abundant and longest-lived bone cells<sup>2,3</sup>, are well known to regulate both bone mass and bone matrix quality through the coordination of osteoblasts and osteoclasts<sup>2,4</sup>. The osteocyte is the topic of interest for new approaches to manage bone fragility in aging, since over time many of these cells become senescent or apoptotic<sup>5,6</sup> and require greater strains to engage anabolic signaling<sup>7-10</sup>. Osteocytes live in a porous network within lacunae connected by canaliculi and can remove and replace (i.e., turn over) bone surrounding this network<sup>2,4,11,12</sup> (**Figure 1A**). There is abundant evidence that aging decreases lacunar and canalicular sizes and connectivity in both rodents and humans<sup>11-16</sup>. These geometric changes imply that bone resorption and mineralization by osteocytes alongside the lacunar-canalicular system (LCS) also shift in aging, with possible impacts to bone quality and mechanosensation<sup>2,4,8,11,17</sup>. However, many fundamental knowledge gaps persist about how osteocytes interact with their surrounding bone tissue and how these processes change in aging.

The impacts of osteocyte peri-LCS turnover (alternatively termed perilacunar or lacunar-canalicular remodeling) on the aging skeleton are uncertain, in part because the percentage of osteocytes that engage in bone resorption or mineralization alongside the LCS is unknown<sup>2,3,11,12</sup>. As witnessed in studies of rodent lactation or PTH treatment, osteocytes can expand lacunae and canaliculi through production of acids as well as enzymes such as cathepsins and matrix metalloproteinases (MMPs)<sup>11,12,18-25</sup>. These pores can then recover to their original size, implying bone re-mineralization 19,24. When mice are injected with fluorochrome labels after weaning, abundant fluorochrome labels are observed<sup>19</sup>. However, labeled osteocyte lacunae are also seen in several studies where rodents were not under applied calcium pressure<sup>26-28</sup>, which suggests that osteocyte LCS mineralization may be a more active and widespread phenomenon than has been previously appreciated. For example, we previously demonstrated that ~60% of randomly-selected lacunae from the femoral midshaft cross-section were labeled with calcein administered 2 days before euthanasia in 5-month and 22-month female C57BL/6 mice<sup>26</sup>. In another study, ~60% of the lacunae in the femoral midshaft cross-section of wild-type male and female C57BL/6 mice at 28-day had calcein labels administered 2 days before euthanasia<sup>28</sup>. Another group found that in the mid cortical cross-section of tibia, ~55% of lacunae showed calcein labels injected 5 days before euthanasia in 2-month male wildtype littermates of MMP13 knockout mice with a mixed C57BL/6 genetic background<sup>27</sup>. These studies differ in age, label dosage, time of injection, region of evaluation, and mouse genetic background. Furthermore, while cortical and cancellous bone differ in their metabolic activities<sup>29–31</sup>, it is unknown whether osteocyte peri-LCS turnover activity varies between these compartments. To investigate the potential impact of peri-LCS turnover on bone quality and

mechanosensation in aging, it is essential to determine the percentage of osteocytes participating in mineralization and resorption in both young adult and aged mice.

The dynamics of peri-LCS turnover are also essential to defining the potential impact of the osteocyte on its surrounding bone. These dynamics have been challenging to study, since LCS bone mineralization and resorption require different bone preparation and analyses. The percentage of osteocytes participating in LCS bone mineralization can be monitored by fluorochrome labeling 11,12,23-28 (Figure 1). The percentage of osteocytes resorbing bone is instead measured through immunohistochemical markers of matrix metalloproteinases and other targets <sup>13,27,28</sup> (Figure 2D). However, there has been a need for an approach to estimate the dynamics of bone turnover from the same bone sections. Serial fluorochrome label injections at short intervals before euthanasia can help address this gap in knowledge (Figure 1B). It is not possible to assess whether an individual mouse had labeled bone that was later removed. However, the average percentage of lacunae showing labels administered at specific time points (e.g., 2 through 16 days) can allow estimation of how long labels persist following deposition. Furthermore, when serial labels are delivered to the same mice, double labels can provide an indication of how long LCS mineralization can occur (Figure 1B). Double labels have thus far only been quantified in lactation studies as evidence of bone infilling following the removal of calcium pressure with weaning<sup>19</sup>. To interpret these peri-LCS turnover dynamics, it is also necessary to assess whether common fluorochrome labels (i.e., calcein and alizarin) show similar retention around osteocyte lacunae.

Another question is whether osteocyte peri-LCS turnover is mechanosensitive and if the dependence of this process on tissue strain changes with aging. Osteocytes are mechanosensitive cells and their signaling activity depends on tissue strain<sup>2,3,7,32,33</sup>. Moreover, osteocytes are less mechanosensitive in aging and require greater strains to engage anabolic signaling<sup>7–10,13</sup>. peri-LCS turnover has the potential to influence osteocyte mechanosensation through altering the shape of the porous LCS network as well as the flow characteristics within it<sup>34–37</sup>. Furthermore, as shown in our recent work using atomic force microscopy, recent LCS mineralization increases the compliance of bone within several hundred nanometers of LCS walls<sup>26</sup>, which would likely contribute towards strain amplification<sup>37</sup>. However, whether peri-LCS turnover influences - or is influenced by - strains experienced by the osteocyte is not yet understood. Since long bones experience tissue strains that vary in direction and magnitude<sup>38,39</sup>, determining how peri-LCS turnover varies throughout femoral cross-sections can help answer first questions about whether this process is associated with tissue strain in young adult and aged mice.

The purpose of this study is to test the hypothesis that aging decreases the percentage of osteocytes engaged in LCS bone mineralization and resorption and alters the dynamics of these processes. This hypothesis was tested by serial fluorochrome labeling and immunohistochemistry studies of cortical and cancellous bones of the femur in 5-month and 22-month female C57BL/6JN mice. We further

hypothesized that the peri-LCS turnover activity depends on variation in tissue strain and that this relationship changes in aging, which we tested by comparing LCS bone mineralization dynamics between femur regions of interest and with distance from the endocortical to periosteal surfaces. Moreover, we hypothesized that peri-LCS turnover activity and impacts of aging would vary for osteocytes located in the lamellar versus non-lamellar compartments of cortical bone, considering previous findings indicating that osteocyte lacunar geometry is influenced by bone structural organization<sup>40,41</sup>.

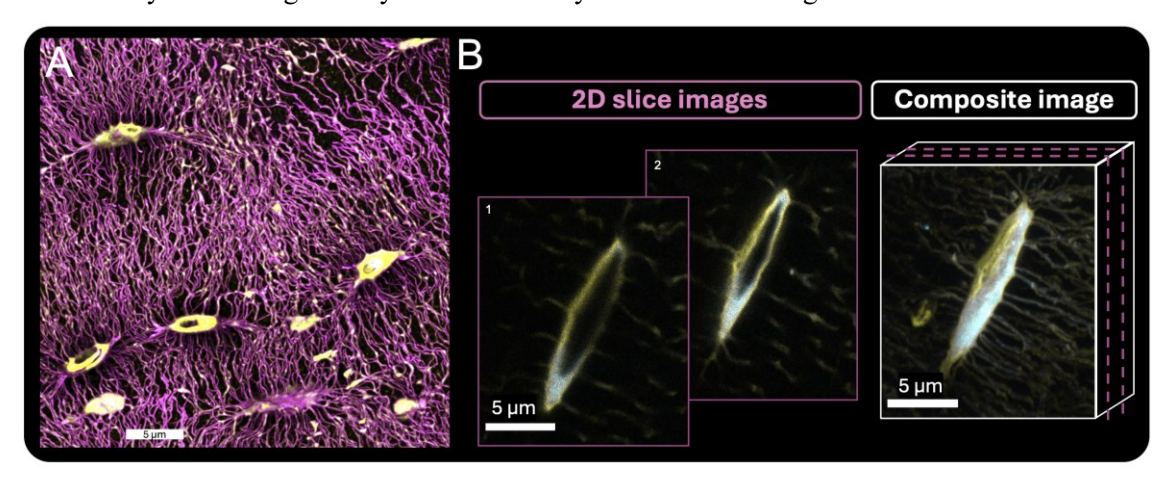


**Figure 1.** Osteocyte lacunar-canalicular system (LCS). A) Osteocytes live in an expansive and intricate network of lacunar holes and canalicular channels. Basic fuchsin staining (magenta, *ex vivo* staining of embedded bones) shows the extensive LCS porosity of cortical bone. Calcein-stained tissue (yellow, *in vivo* fluorochrome injection 2 days before euthanasia) indicates bone mineralization. B) Osteocyte lacunae can show double labels when administered at short timepoints before euthanasia. *In vivo* serial fluorochrome labeling (calcein in yellow, 2 days before euthanasia; alizarin in blue, 8 days before euthanasia) in a female 5 mo C57BL/6JN mouse reveals double-labeled lacunae. Figure 1 generated by G. Vahidi and reprinted with permission from Current Osteoporosis Reports.

#### 2.0 Materials and Methods

#### 2.1 Animals

All animal procedures were approved by Montana State University's Institutional Animal Care and Use Committee. 5 months old young adult (5 mo, n = 20) and 22 months old early-old-age (22 mo, n=16) female C57BL/6JN mice from the National Institutes of Aging colony were utilized in this study. Mice had a minimum of two weeks to acclimatize to the MSU animal facility before the beginning of the label studies. Mice had *ad libitum* access to water and standard chow. Each mouse was administrated two intraperitoneal injections of fluorochrome labels, calcein (20 mg/kg, i.p.) and alizarin (30 mg/kg, i.p.) at two specific dates that varied for each group of mice. The goal was to collect data for injection dates that include 16d, 8d, 4d, or 2d before the euthanasia, while each group of mice received only two injections with specific timing and sequence of the injections (**Figure 2A**). For example, a group of mice received 2d calcein and 4d alizarin whereas another group received 2d alizarin and 16d calcein. To ensure that label identity was not confounded with the specific time points, some mice received the calcein injection first and the alizarin injection second. Other mice received label injections in the opposite order. No

significant effects of label type (i.e., alizarin or calcein) were observed on the percentage of labeled lacunae (**Figure S1**). Therefore, we aggregated the label identity data, pooling alizarin and calcein data for each label date with n = 4-16 sample per age/label date group. Labeling group sample sizes were as followed: in 5 mo group, mice received labels at 2d (n=16), 4d (n=6), 8d (n=10), or 16d (n=8) before euthanasia; in 22 mo group: mice received labels at 2d (n=10), 4d (n=4), 8d (n=9), or 16d (n=9) before euthanasia. All mice received two labels. Mice were euthanized at 5 or 22 months of age via isoflurane inhalation followed by cervical dislocation.

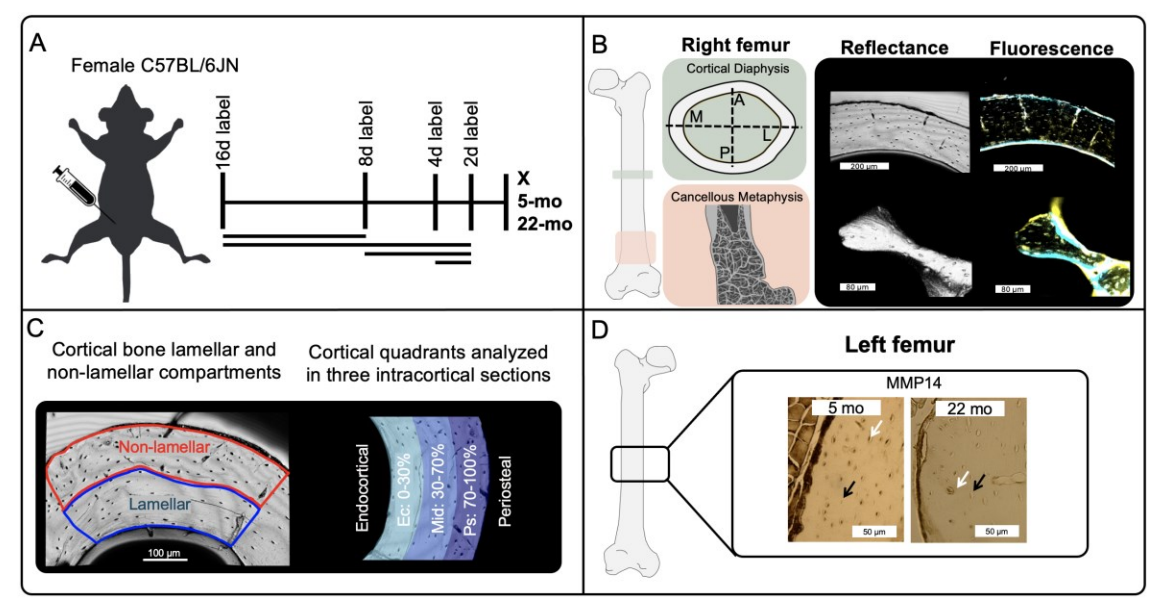


**Figure 2.** Schematic of study experimental procedures. A) Each group of mice received intraperitoneal injections of fluorochrome labels at two specific dates (16d, 8d, 4d, or 2d) before euthanasia at either 5 months or 22 months of age. B) The femur diaphysis (A/P/M/L regions) and distal metaphysis were imaged with a confocal microscope in fluorescence and reflectance modes to evaluate labeled and unlabeled lacunae on the bone surface. Representative images show 2d calcein labels (yellow) and 8d alizarin labels in (blue) for 5 mo mice. C) Cortical bone was visually divided into lamellar and non-lamellar compartments for further analyses. Cortical bone was also divided into three intracortical sections for analysis based on variation in tissue strain. D) MMP14+ lacunae were counted to quantify perilacunar bone resorption for cortical bone. White arrows show MMP14+ lacunae and black arrows show unlabeled lacunae.

#### 2.2 Sample preparation

Right femurs were harvested, cut transversely in half at the femoral midshaft, and then the proximal and distal fragments were embedded in non-infiltrating epoxy (Epoxicure 2, Buehler) without any ethanol dehydration steps, air-drying, or fixation. The proximal side of the mid-shaft cross-section was used for cortical bone studies. The embedded distal halves were cut through the sagittal plane to expose femoral metaphysis for cancellous bone studies, using a low-speed diamond saw (Isomet, Buehler). All samples were polished to achieve a mirror-like finish, using wet silicon carbide papers (600 and 1000 grits, Buehler) followed by Rayon fine cloths and alumina pastes (9, 5, 3, 1, 0.5, 0.3, and 0.05 µm, Ted Pella, Inc.).

Left femurs were harvested and immediately fixed with 10% neutral-buffered formalin, decalcified with EDTA disodium salt dihydrate, dehydrated in a graded ethanol series, embedded in paraffin, transversely cut at femoral midshaft, and each half was serially sliced into 5-micron-thick horizontal cortical diaphysis sections for immunohistochemistry analyses.

154155156

157

158

159

160161

162

163

164

165

166

167

168

169

170

171

172

173

174

175

176

177

178

179

180

181

182

183184

151

152

153

#### 2.3 Analysis of bone-mineralizing osteocytes via fluorochrome labeling

An inverted confocal laser scanning microscope (CLSM- Leica Stellaris DMI8, Wetzlar, Germany) was used to identify labeled and unlabeled osteocyte lacunae using a 20× lens (dry, 0.75 NA, 0.78 μm lateral resolution) at 600 Hz speed with a 1024 × 1024 resolution, and pinhole set at 1 Airy unit. Calcein labels were visualized using an excitation wavelength of 488 nm and emission wavelength of 500-540 nm. Alizarin labels were visualized using an excitation wavelength of 561 nm and emission wavelength of 600-645 nm. The reflectance mode was used to image the bone surface, allowing measurement of the total number of lacunae. Then, fluorescence images were taken from the same site to measure the number of fluorochrome-labeled lacunae. The percentage of fluorochrome-labeled lacunae on the bone surface was calculated as the ratio of labeled lacunae to all lacunae on the bone surface (Figure 2B). All images were collected in z-stacks (~30 μm thickness, 0.6 μm between slices) to confirm whether the surfacevisible lacunae were labeled or not in 3D space. For each channel (alizarin and calcein) in every image, we calculated the mean and standard deviation of the grayscale intensity using ImageJ<sup>42</sup>. Then, we determined a minimum intensity value by adding 1.5 times the standard deviation to the mean grayscale intensity. Using Imaris 9.3, we set the minimum threshold of fluorescent intensity for each channel in each image to this calculated value. The percentage of bone-mineralizing osteocytes (i.e., labeled lacunae) was measured for cortical bone within anterior (A), posterior (P), medial (M) and lateral (L) regions of interest (ROIs) at the femoral midshaft (Figure 2B). For each ROI, this percentage was also separately reported for lamellar and nonlamellar compartments of cortical bone, which were visually identified from reflectance images, (Figure **2C**), to assess the impact of different bone types on bone-mineralizing osteocytes. We also investigated the effect of natural strain variations that exist in cortical femur diaphysis<sup>43</sup> on osteocyte bone mineralization activity. First, we compared the percentage for bone-mineralizing

osteocytes between anterior (close to femur loading axis) and medial (close to femur neutral axis) ROIs (**Figure 6A**). These quadrants were chosen because the anterior femur experiences tensile strains while the medial quadrant experiences consistently lower strains. By contrast, the posterior and lateral quadrants experience more complicated stresses <sup>43</sup>. Because tensile strains increase from the endocortical to periosteal surfaces of the anterior quadrant <sup>43</sup>, we also compared the percent of bone mineralizing lacunae with respect to intracortical position with relation to the endocortical surface: 0-30%, 30-70%, and 70-

100% of the cortical thickness (**Figure 2C**). We referred to the sections as Ec (endocortical, 0-30%), Mid (middle, 30-70%), and Ps (periosteal, 70-100%). These same regions were also assessed for the medial quadrant, which has much less intracortical stress variation<sup>43</sup>. For analyses of cancellous bone, multiple trabecular regions (**Figure 2B**)) were selected from the metaphysis of each mouse, exposed by sagittal sectioning of the femur's distal half. The percentage of labeled lacunae was calculated for each trabecular region (**Figure 2B**)), and then the mean and standard deviation of all trabecular regions in each mouse were reported. Custom Matlab codes were employed for these analyses (MATLAB codes available on GitHub repository: <a href="https://github.com/Ghazal-vhd/LCST\_LabelCount\_Femur.git">https://github.com/Ghazal-vhd/LCST\_LabelCount\_Femur.git</a>). These codes counted the number of lacunae on the bone surface from reflective images and the number of labeled lacunae from fluorescence images within regions of interest defined by the user, calculating the percentage of labeled lacunae for both cortical and cancellous regions.

During data collection, the laser for the Leica Stellaris DMI8 was updated from a diode laser to a white light laser while the detectors remained unchanged. Emission and excitation ranges were kept similar, but adjustments were made to the new laser's settings such as gain and power to ensure a uniform image production. All images, both pre- and post-update, were normalized to their respective mean and variable intensity, as previously described. Our analysis revealed no discernible impact of the laser change (included as a blocking factor in all the statistical models) on any outcomes.

The high-resolution images in **Figure 1** were from cortical femurs of a 5 months old female C57BL/6JN mouse. This mouse received alizarin injection 8 days and calcein injection 2 days before euthanasia. Both femurs were dehydrated with degraded ethanol series and embedded in polymethyl methacrylate. The right femur was stained with basic fuchsin during the dehydration process<sup>44,45</sup> and used for **Figure 1A**. Images were taken with a 63×-oil immersion objective using the same Leica Stellaris DMI8 confocal microscope.

## 2.4 Analysis of osteocyte matrix metalloproteinase expression by immunohistochemistry

Paraffin-embedded left distal femurs were used for immunohistochemistry (IHC) following previously published protocols<sup>46</sup>. Slides were dewaxed and rehydrated (ethanol and distilled water series). Subsequently, the slides were incubated in Innovex Uni-Trieve retrieval solution (329ANK, Innovex Animal IHC kit) for 30 min in a 65 °C water bath. Slides were blocked with the Innovex kit's Fc-block and Background Buster, each for 45 minutes in the room temperature. Next, samples were incubated with the primary antibodies (1:100 anti-MMP14; ab38971 both diluted in PBS) for one hour at room temperature and subsequently with secondary antibodies (Linking Ab, 329ANK) and peroxidase (HRP) enzyme for 10 minutes each at room temperature. Following this, the slides were treated with DAB working solution at room temperature for 5 minutes, washed with PBS, and mounted with Innovex

Advantage permanent mounting media. Negative controls were conducted by replacing the primary antibody with rabbit IgG at the same concentration. Images were captured using a Nikon E-50i microscope (Nikon, Melville, NY, SA) with dry 4× (full cortical cross-section) and dry 20× (each cortical ROI) objectives (**Figure 2D**). For MMP14 comparisons, we had n=18 and n=20 mice for 5 mo and 22 mo groups, respectively. The mean percentage of MMP14+ osteocyte lacunae for each cortical ROI (A, P, M and L) was quantified using ImageJ. This percentage was not characterized in cancellous bone due to sample availability.

### 2.5 Analysis of lacunar geometry via scanning electron microscopy

A subset of samples (n=6 per age) was coated with a thin layer of carbon for lacunar geometrical analyses via backscattered scanning electron imaging (Zeiss Supra 55VP field emission SEM, 15 kV, 60  $\mu$ m aperture size, 400× magnification, and 9.1 mm working distance). Samples were mounted in a custom holder that ensures flat surfaces at the same height<sup>47</sup>. Images were collected for the anterior ROI. A custom Matlab code was used to calculate lacunar geometry for the lamellar compartment of cortical bone<sup>16</sup>. An area filter removed objects smaller than ~5  $\mu$ m<sup>2</sup> and larger than ~200  $\mu$ m<sup>2</sup>. Them, pores smaller than ~70  $\mu$ m<sup>2</sup> were considered lacunae. The following parameters were calculated: lacunar porosity (%), lacunar number density (#/ mm²), lacunar area ( $\mu$ m², the area of an ellipse fitted to the segmented 2D osteocyte lacunae), lacunar major and minor axes ( $\mu$ m), and lacunar circularity (i.e., ratio of minor to major axis of the fitted ellipse, where a value of 1 indicates a perfect circle). We also assessed differences in lacunar geometry between labeled and unlabeled lacunae for a small subset of samples that were labeled 8 days and 2 days before euthanasia in both 5 mo (n=4) and 22 mo (n=3) groups. We overlapped the SEM images with CLSM maps of labeled and unlabeled lacunae to test whether lacunar area differs between bone-mineralizing and non-bone-mineralizing osteocytes.

## 2.6 Statistical analyses

Mixed model ANOVA, with mouse as the random effect, tested whether percentage of bone-mineralizing osteocytes depended on the fixed effects of age, tissue strain (i.e., A/P/M/L ROIs), label date, or interactions of these variables for cortical bone. Additional mixed model ANOVAs were utilized for lamellar and non-lamellar cortical compartments. For the comparisons of intracortical distances (0-30%, 30-70%, and 70-100%), the two age groups were separated and for each age, mixed model ANOVA with mouse as a random effect was used to test if the percentage of bone-mineralizing osteocytes (for 2d and 16d labels, separately) depended on the fixed effects of ROI, intracortical distance, or their interactions. For cancellous bone, two-way ANOVA was employed to test if age, label date, and the interaction of these factors affect percentage of bone-mineralizing osteocytes. Since the confocal laser

was changed mid-study, this was included as a blocking factor in these models. Because the laser change was not a significant effect for any measure, this blocking factor was removed, and models were rerun. Mixed model ANOVA with mouse as a random effect was used to test if the percentage of MMP14+ lacunae depends on age, ROI, or their interactions. We tested the effect of age on the measurements of lacunar geometry from SEM using a two-sample t-test. For the lacunar area differences between labeled and not labeled lacunae, we employed mixed model ANOVA with mouse as the random effect and age and label status (yes or no) as fixed effects. For all models, model residuals were checked for satisfaction of assumptions of normality and homoscedasticity. Dependent variables were log-transformed if necessary to satisfy these assumptions. Significance was set a priori to p < 0.05. Significant interactions between factors were followed up with Tukey post hoc tests. All analyses were performed with Minitab (20).

#### 3.0 Results

## 3.1 Aging decreases the number of osteocytes participating in peri-LCS turnover

Osteocyte participation in mineralizing their immediate surrounding was highly abundant in the cortical and cancellous femur of young adult C57BL/6JN mice. However, with aging, there was a large decrease in the percentage of recently bone-mineralizing osteocytes (i.e., 2d labeled lacunae) in both cortical and cancellous regions. In cortical bone of 5 mo mice, 80% of lacunae showed 2d labels, while in 22 mo mice, 50% of lacunae had 2d labels. Thus, from 5 mo to 22 mo, there was a 38% reduction in the percentage of 2d labeled lacunae in cortical bone (p < 0.001, Figure 3A & C). In cancellous bone of 5 mo mice, 85% of the lacunae had 2d labels, while in 22 mo mice, 58% of lacunae showed 2d labels.

Therefore, aging reduced the percentage of 2d labeled lacunae by 32% (p < 0.001, Figure 3B & D).

The percentage of double-labeled lacunae (i.e., positive for both 2d and 16d labels) was also abundant in 5 mo femurs, with more than 45% of the lacunae in cortical bone and 60% of lacunae in cancellous bone having double-labels. The percentage of double-labeled lacunae decreased with aging. In 22 mo mice, 26% of lacunae in cortical bone and 10% of lacunae in cancellous bone showed double-labels. Thus, from 5 mo to 22 mo, there were 45% (p = 0.05, Figure S2) and 85% (p < 0.001, Figure S2) fewer double-labeled lacunae in cortical and cancellous tissues, respectively.

The percentage of MMP14+ lacunae (i.e., positive for a marker of bone resorption) was also highly abundant in femoral cortical bone of 5 mo mice. For these young adult mice, more than 75% of cortical lacunae were positive for MMP14 (**Figure 3E & F**). With increased age, there was a significant decrease in the percentage of MMP14+ lacunae (22 mo vs 5 mo: -10%, p < 0.001). The percentage of MMP14+ lacunae was not characterized in cancellous bone due sample availability and future investigations would benefit from this analysis.

Our data showed greater variability in the percentage of bone mineralizing osteocytes in both cortical and cancellous bones of 22 mo mice compared to 5 mo mice (SD comparisons of 22 mo vs 5 mo groups; Cortical: +60%, p < 0.05; Cancellous: +230%, p < 0.001; p values are from Bartlett and Levene tests of equality of variances between the two groups). This is consistent with observations of higher variability in bone matrix quality and LCS characteristics with aging  $^{16,48-52}$ .



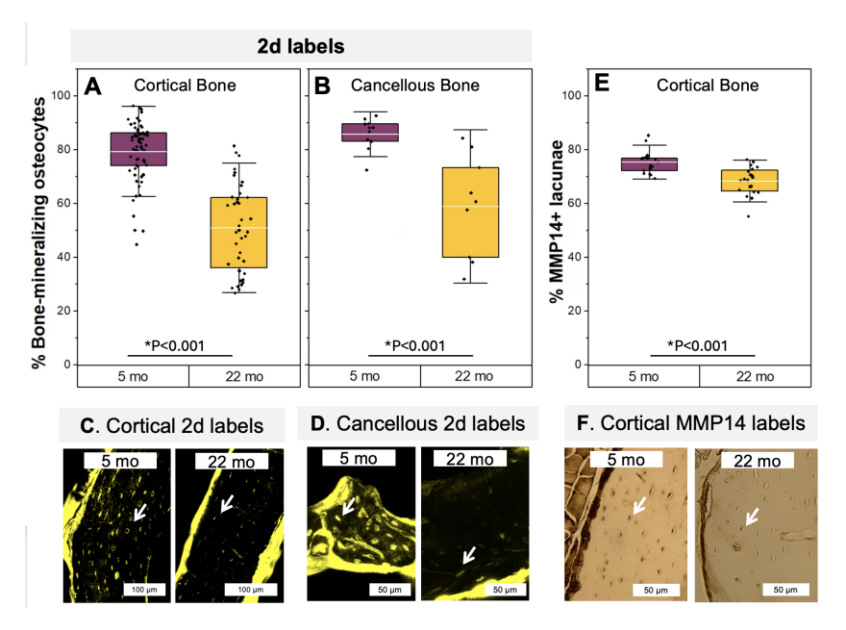


**Figure 3.** The effect of aging on cortical and cancellous osteocyte bone mineralization and resorption. Bone-mineralizing osteocytes were less abundant with aging in both A) cortical and B) cancellous bone. Only 2d labels are shown here. C & D) Representative fluorescence images of calcein labels for 5 mo and 22 mo mice shown. For 2d label comparisons, we had n=16 and n=10 mice for 5 mo and 22 mo groups, respectively. E & F) Aging also decreased the percentage of MMP14+ lacunae in cortical bone. White arrows show 2d labeled (yellow) or MMP14+ lacunae. All data are reported as percentages (labeled lacunae/all lacunae). For MMP14 comparisons, we had n=18 and n=20 mice for 5 mo and 22 mo groups, respectively. Boxplots represent mean value (cross), interquartile range (box), minimum/maximum (whiskers), and symbols representing all data points. All p-values correspond with results of the omnibus ANOVA test. \* indicates a significant effect of age.

#### 3.2 Aging alters peri-LCS turnover dynamics more for cancellous than for cortical bone

The percentage of labeled lacunae decreased for injection dates further from euthanasia. For cancellous bone from 5 mo mice, the percentage of 16d labeled lacunae was 29% (p < 0.001) lower compared to 2d labeled lacunae (**Figure 4E & G**). By contrast, at 22 mo, the percentage of 16d labeled lacunae was 81% (p < 0.001) lower compared to 2d labeled lacunae (**Figure 4F & H**), suggesting that the rate of label disappearance is higher with increased age in cancellous bone. In cancellous bone of both 5 mo and 22 mo groups, the percentage of 8d labels decreased compared to 2d labels (5 mo: -15%, p < 0.001, 22 mo: -39%, p < 0.001), while the percentage of 4d labels was not different from 2d labels (p > 0.05).

In cortical bone of 5 mo mice, there were 44% (p < 0.001) fewer lacunae labeled at 16d compared to 2d (**Figure 4A & C**). For 22 mo mice, there were 61% (p < 0.001) fewer 16d labeled lacunae compared to 2d labeled lacunae (**Figure 4B & D**), implying that in cortical bone, peri-LCS turnover undergoes a more modest change with aging compared to cancellous bone. There were 47% (p < 0.001) fewer lacunae with 8d labels compared to 2d labels in cortical bone of 22 mo mice, however, 8d label percentage was not different from 2d label percentage in 5 mo mice (p > 0.05). The percentage of 4d labels was not different from 2d labels (p > 0.05 for either age).

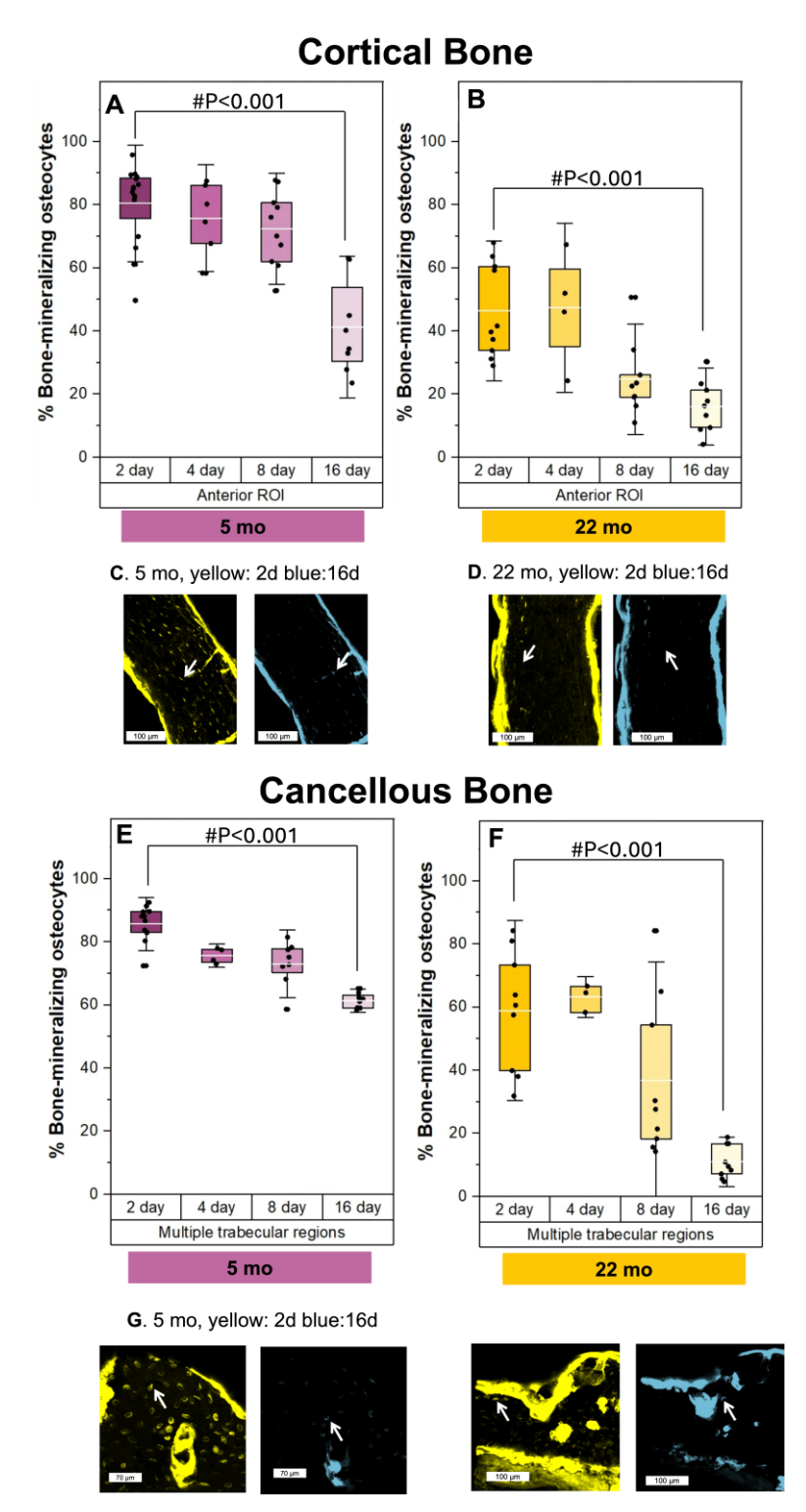


**Figure 4.** The effect of aging on the dynamics of osteocyte bone turnover. A-D) In cortical bone, compared to 2d labels, labels administrated 16d before euthanasia were 44% and 61% less abundant in 5 mo and 22 mo mice, respectively. E-H) In cancellous bone, compared to 2d labels, 16d labels were 29% and 81% less abundant in 5 mo and 22 mo mice, respectively, suggesting aging alters peri-LCS turnover dynamics more for cancellous than for cortical bone. Data for other ROIs of cortical bone are shown in supplementary information. All data are reported as percentages (labeled lacunae/all lacunae). Representative fluorescence images of 2d labels (calcein label is shown in

yellow) and 16d labels (alizarin label is shown in blue) for 5 mo and 22 mo samples shown in both cortical and cancellous tissues. White arrows show 2d labeled lacunae. For the 5 mo group, sample sizes were: 2d (n=16), 4d (n=6), 8d (n=10), and 16d (n=8). For 22 mo group, sample sizes were: 2d (n=10), 4d (n=4), 8d (n=9), and 16d (n=9). Boxplots represent mean value (cross), interquartile range (box), minimum/maximum (whiskers), and symbols representing all data points. All p-values correspond with results of the omnibus ANOVA test. # indicates a significant effect of injection date.

# 3.3 The impact of aging on peri-LCS turnover is similar between lamellar and non-lamellar compartments of cortical bone

Since osteocyte lacunar geometry depends on the bone structural organization (e.g., lamellar vs non-lamellar bone) $^{40,41}$ , we further divided the cortical bone into lamellar and non-lamellar compartments. We observed a similar age-induced decline in the percentage of bone-mineralizing osteocytes in both lamellar (for M ROI, 22 mo vs 5 mo: -49%, p < 0.001) and non-lamellar (for M ROI, 22 mo vs 5 mo: -46%, p < 0.001) bones (**Figure 5**, **Figure S3** shows data for all ROIs). Similarly, in both age groups, 16d labels were significantly less abundant compared to 2d labels in both lamellar (for M ROI, 5 mo 16d vs 2d: -40%, 22 mo 16d vs 2d: -62%, all p < 0.001) and non-lamellar compartments (for M ROI, 5 mo 16d vs 2d: -45%, 22 mo 16d vs 2d: -60%, all p < 0.001) of cortical bone (**Figure 5**).

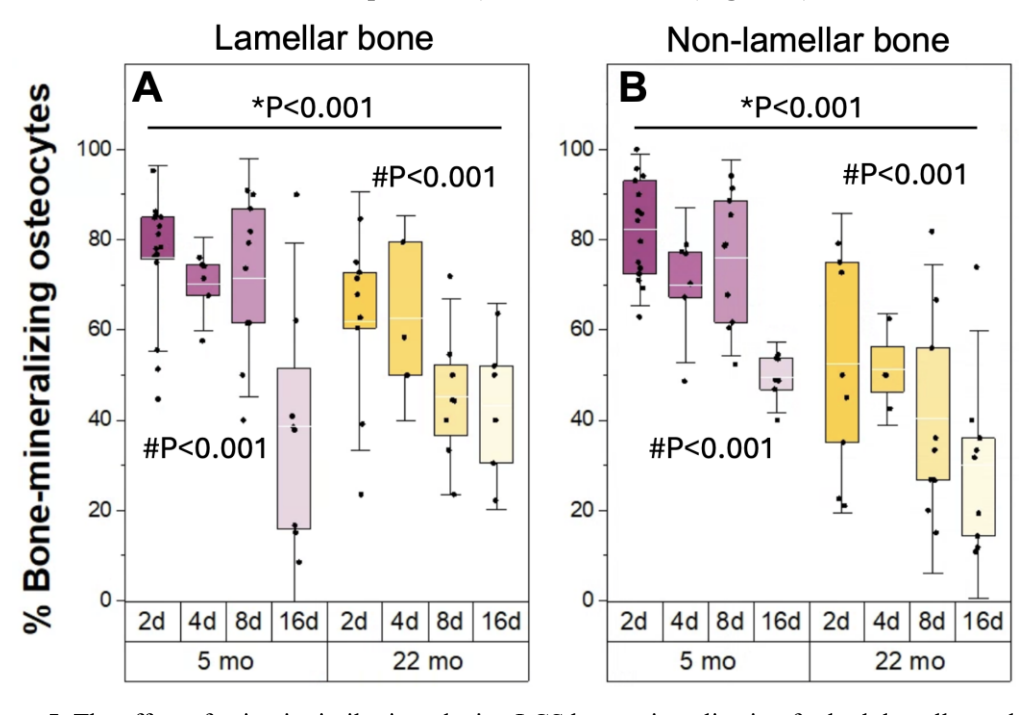


**Figure 5.** The effect of aging is similar in reducing LCS bone mineralization for both lamellar and non-lamellar bone. For both A) lamellar and B) non-lamellar compartments of cortical bone, aging reduced the percentage of bone-mineralizing osteocytes. For both types of tissues, 16d labeled lacunae were significantly less abundant compared to 2d labeled lacunae regardless of the age group. Data are shown for the medial ROI, where we consistently observed comparable amounts of both lamellar and non-lamellar bone across all mice. In contrast, the size of lamellar and non-lamellar bone regions varied significantly in the other ROIs, and some mice did not have non-lamellar bone in the anterior ROI. Results for all ROIs are presented in Figure S3. All data are reported as percentages (labeled lacunae/all lacunae). Boxplots represent mean value (cross), interquartile range (box),

minimum/maximum (whiskers), and symbols representing all data points. All p-values correspond with results of the omnibus ANOVA test. \* indicates a significant effect of age. # indicates a significant effect of injection date.

352

353

354

355

356

357

358359

360

361362

363

364

365

366367

368

369

370

371

372373

374

375

376377

378

379

380

381

382

383384

## 3.4 The relationship between peri-LCS turnover and cortical quadrant and intracortical location of osteocytes depends on age

In mouse femur cross-section, the strain environment is distinct between anterior (A), posterior (P), medial (M), and lateral (L) ROIs based on their position with respect to the femur loading axis and natural axis (**Figure 6A**)<sup>43</sup>. Because the osteocyte is a mechanosensitive cell<sup>38,39</sup>, we compared LCS bone mineralization and resorption for these ROIs. In 5 mo mice, we did not find a relationship between LCS turnover dynamics and the position of the osteocytes in distinct strain environments of the femur cortex (p = 0.815, **Figure 6B**). However, in 22 mo mice, we found an association between the peri-LCS turnover dynamics and the position of the osteocytes in different ROIs of cortical femur (age and ROI interaction p < 0.001). Osteocytes in the medial ROI of aged femurs (close to femur neutral axis) had higher participation in mineralizing their surrounding compared to those in the other three ROIs (e.g., M vs A: +44% p<0.001, **Figure 6B**). There were no differences in the percentage of labels among anterior, posterior, and lateral ROIs. Notably, the decay of 16-day labels exhibited a slower pace in the medial ROI in comparison to the others. ROI did not impact the percentage of MMP14+ lacunae in 5 mo or 22 mo mice (p = 0.7).

Ascenzi et al. demonstrated that for the anterior ROI of the mouse femur, intracortical tissue tensile strains increases with distance from the centroid<sup>43</sup>. However, in the medial ROI, which is close to the femur neutral axis, strains are lower and are relatively unaffected by distance from the centroid. The intracortical strain distribution is more complex for posterior and lateral ROIs<sup>43</sup>. Therefore, we divided anterior and medial ROIs with simpler and more distinct strain distribution patterns into three sections with respect to the position between the endocortical and periosteal surfaces. Distance sections included Ec: 0-30%, Mid: 30-70%, and Ps: 70-100% (Figure 6A). There were no significant interactions between ROI and distance for either 5 mo or 22 mo mice. In 5 mo mice, both 2d labeled and 16d labeled lacunae percentages were influenced by the intracortical position but not by ROI. At this age, posthoc testing reveals that the lacunae closest to the periosteal surface (Ps: last 70-100% of cortical thickness) had a smaller percentage of 2d labels compared to the other two distances (Ec = Mid > Ps, p = 0.017, Figure **6C**). There were fewer 16d-labeled lacunae within the middle distance (Mid: 30-70% of cortical thickness) compared to other distances (Ec = Ps > Mid, p = 0.038, **Figure 6D**). Differences in the percentage of labeled lacunae with intracortical position were more pronounced for 22 mo mice. At this age, lacunae within the middle intracortical distance had lower percentage of 2d labels compared to other the other distances (Ec = Mid > Ps, p = 0.001, Figure 6E). Periosteal distance section in 22 mo mice

showed the highest percentage of 16d labels compared to the other distances (Ec = Mid < Ps, p < 0.001, **Figure 6F**).

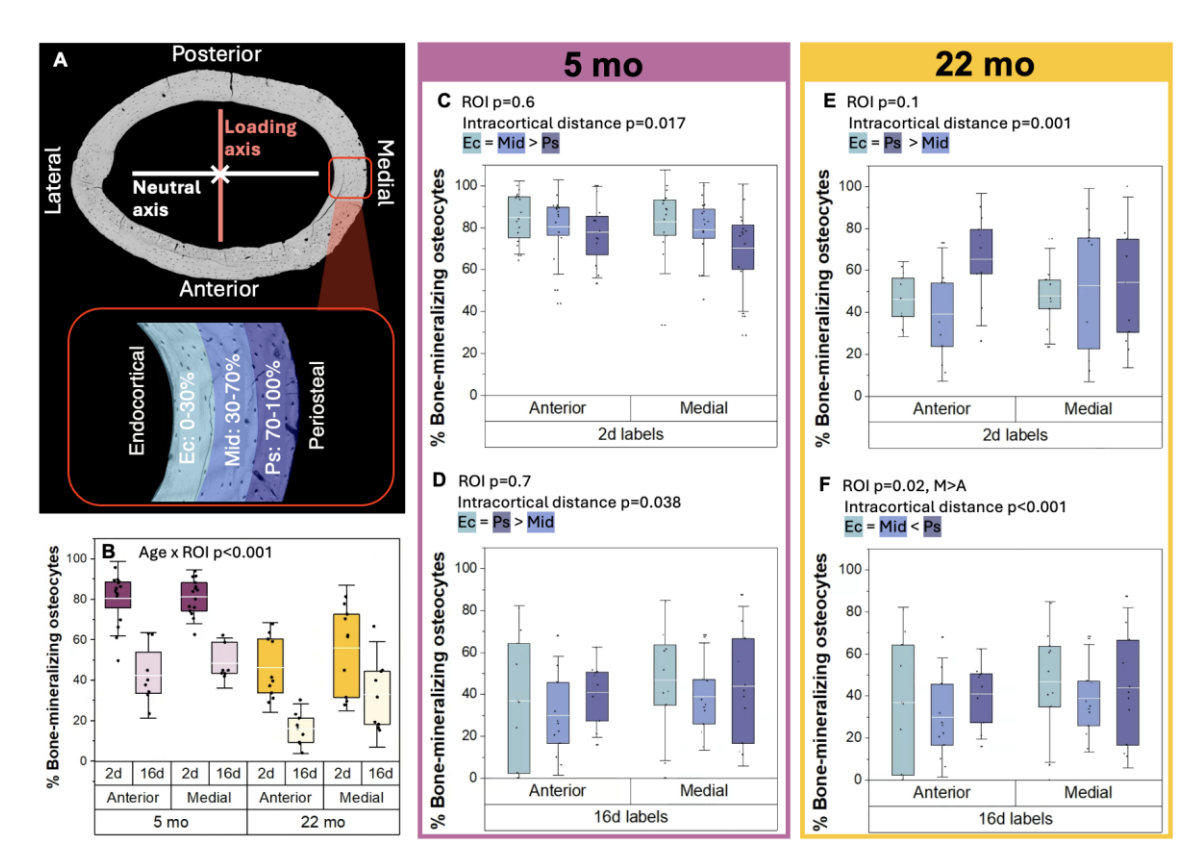


**Figure 6.** Associations between tissue strain and osteocyte participation in LCS bone mineralization. A) Schematic of anterior, posterior, medial, and lateral ROIs and their position with respect to the femur loading axis and natural axis. Anterior and medial ROIs were divided into three distance sections from the endocortical surface (0-30%, 30-70%, and 70-100% of cortical thickness) for further investigation of whether osteocyte bone mineralization is associated with differences in tissue strain. B) In 5 mo mice, anterior vs medial ROI did not impact the percentage of bone-mineralizing osteocytes. However, for 22 mo mice, lacunae in the medial ROI had the highest percentage of labeling compared to all ROIs. C) In 5 mo mice, the percentage of 2d labeled lacunae was lowest in the region closest to periosteal surface, for both anterior and medial ROIs. D) For 5 mo mice, the percentage of 16d labeled lacunae was lowest in the middle intracortical region, for both anterior and medial ROIs. E) In 22 mo mice, the percentage labeling differences between intracortical sections were larger. Middle intracortical section in 22 mo mice had fewer 2d labeled lacunae compared to other sections in both anterior and medial ROIs. F) In 22 mo mice, the percentage of 16d labeled lacunae was highest in the region closest to periosteal surface and 16d labels consistently showed higher percentages in the medial ROI compared anterior ROI. Data are reported as percentages (labeled lacunae/all lacunae). Boxplots represent mean value (cross), interquartile range (box), minimum/maximum (whiskers), and symbols representing all data points. All p-values correspond with results of the omnibus ANOVA test.

#### 3.5 Osteocytes with active peri-LCS turnover have larger lacunae

We conducted a quantitative analysis of backscattered SEM images at the anterior ROI of femoral cross-sections to assess whether lacunar geometry changes with aging and the recency of labeling. Since lacunar geometry differs between lamellar and non-lamellar bones, and the relative size of these regions changes in aging, we restricted our analyses to lamellar bone. We chose the anterior ROI because,

compared to other ROIs, it was consistently composed mostly of lamellar bone. Compared with 5 mo mice, 22 mo mice had decreased cortical lacunar porosity (-27%, p=0.037) but not lacunar number density (p=0.35) (**Figure S4**). Older mice also had smaller lacunae, as seen by smaller lacunar area (-22%, p=0.02), major axis (-12%, p=0.045), minor axis (-15%, p=0.05) (**Figure 7A-B, Figure S4**). No changes were seen in lacunar circularity with age. It is noted that previous work found that 2D SEM analysis is insufficient to detect expected increased sphericity in lacunae with aging <sup>16</sup>.

We also asked whether lacunar size differs between labeled and unlabeled lacunae by overlaying SEM and CLSM maps of the anterior region at the cortical midshaft femur for only a subset of SEM samples that had 2d and 8d labels. The distribution of labeled lacunar sizes is approximately normal for both 5 mo and 22 mo mice (**Figure 7 B & E**). By contrast, the sizes of unlabeled lacunae show closer to a uniform distribution for both ages. Our data suggest that recent peri-LCS turnover increases lacunar area (**Figure 7 B & E**). Labeled lacunae had larger mean (+11% in 5 mo and +14% in 22 mo, both p = 0.05) and median lacunar areas compared with unlabeled lacunae (**Figure 7 A & D & G**).

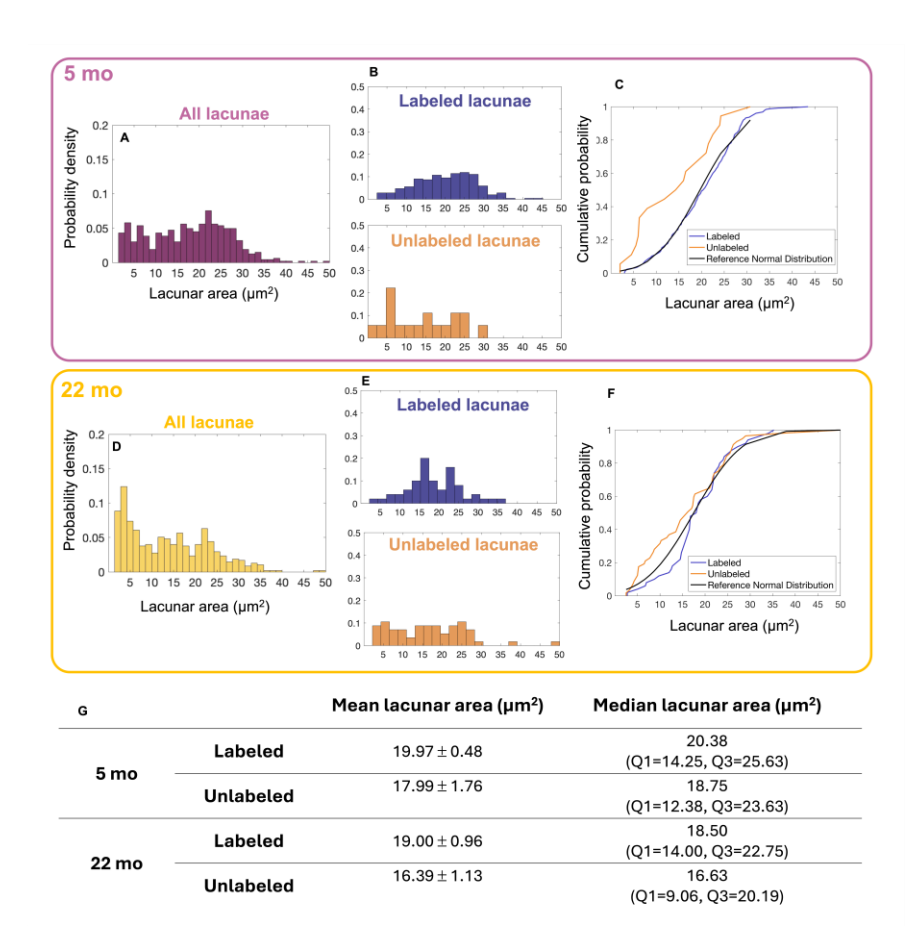


**Figure 7.** Osteocytes with active mineralization have larger lacunae. Overlayed SEM and CLSM maps show that A-G) labeled lacunae had larger areas compared to unlabeled lacunae in both age groups. A-C) The distribution of lacunar sizes in 5 mo mice (n=4) was approximately normal for labeled lacunae (i.e., 2d labeled and/or 8d labeled). However,

the distribution of lacunar sizes for unlabeled lacunae (i.e., no 2d or 8d labels) deviated from normality. D-F) In 22 mo mice (n=3), labeled lacunae had a distribution of lacunar sizes that was closer to normal whereas unlabeled lacunae did not have a normal distribution. The distributions in E-F are depicted as probability density function as well as cumulative density function plots. Data in table are represented as mean with standard error and median with first and third quartiles.

#### 4.0 Discussion

427

428

429

430

431

432

433

434

435

436

437

438439

440

441442

443

444445

446447

448

449450

451452

453

454

455456

457

458459

460

461

Osteocyte lacunar-canalicular system (LCS) turnover has been of high research interest as a possible contributor to age-related changes in bone fracture resistance <sup>2,3,11,12,17,26</sup>. Extensive evidence indicates that age reduces osteocyte viability and mechanosensitivity<sup>7–10,13,17</sup> and truncates lacunar and canalicular dimensions and connectivity<sup>11–16</sup>. These changes imply that there is a decrease in peri-LCS turnover in aging, which could have impacts to osteocyte mechanosensitivity and bone matrix quality<sup>11,13,14,17,27,28</sup>. At present, however, more questions than answers exist about where and how often osteocytes remove and replace their surrounding bone. Our study aimed to test the hypothesis that fewer osteocytes participate in LCS bone mineralization and resorption in aging C57BL/6JN female mice (5 mo vs 22 mo). In this work, we find that aging reduces cortical and cancellous osteocyte participation in both perilacunar bone mineralization and resorption, in a manner that likely depends on tissue strain.

The osteocyte is known to remove and replace bone surrounding the LCS in response to perturbations in calcium homeostasis (e.g., lactation, PTH)<sup>11,12,18-25</sup>, However, the participation of osteocytes in peri-LCS turnover outside of calcium pressure is uncertain<sup>11</sup>. We utilized serial fluorochrome labeling to estimate where, when, and how often osteocytes turn over their surrounding bone. Each mouse in this study was administered two fluorochrome labels at different times before euthanasia. We find that osteocyte bone turnover is highly prevalent in young adult mice, in both cortical and cancellous bone. Over 80% of osteocytes show fluorochrome labeled lacunae administrated 2 days before euthanasia. These numbers decrease to around 45% at 16 days before euthanasia, suggesting rapid bone turnover (Figure 4). Since label disappearance is an indirect indicator of bone resorption, we stained decalcified sections from the contralateral femurs for MMP14. Previous studies suggest that under conditions of elevated PTH signaling, osteocytes can acidify and demineralize bone matrix using matrix-degrading enzymes such as cathepsins and matrix metalloproteinases, in a process known as osteocytic osteolysis 19,22,27. We show that in 5 mo mice, a comparable percentage of osteocytes are positive for bone resorption (i.e., MMP14-positive) as for bone mineralization (i.e., fluorochrome-labeled) (Figure 3). Together, these data suggest that osteocytes in the young adult murine skeleton engage in a pattern of frequent, near-daily bone mineralization along the LCS, coupled with frequent bone resorption events.

Aging has established deleterious impacts on the osteocyte. With increased age, osteocyte apoptosis and senescence both increase while autophagy decreases<sup>5,53</sup>. Aging reduces the size of lacunae and canaliculi, as well as the connectivity of this network<sup>11–16</sup>. These changes imply, but do not determine,

that peri-LCS turnover also changes with age. Here, we report that aging also reduce LCS bone mineralization and, to a lesser extent, resorption activities. Compared with 5 mo mice, 22 mo mice have a 58% decrease in the percentage of 2d labeled lacunae and a 10% decrease in the percentage of MMP14+ lacunae in cortical bone (**Figure 3**). The rate of decrease in label percentage from 2d to 16d in cortical bone is similar across ages. These data suggest that while the number of osteocytes participating in peri-LCS turnover decreases with aging, active osteocytes of different-aged cortical bone may have a characteristic time span of bone deposition before resorption events. The characteristics of peri-LCS turnover did not differ between lamellar and non-lamellar bone at either 5 or 22 mo ages. This is an important finding, since bone organization changes with aging and previous studies have shown that aging affects LCS geometry and density differently in these bone types 40,54–56. These data add to our understanding of aging bone biology by providing the first evidence that peri-LCS turnover activity declines with aging.

Osteocytes reside within cortical and cancellous bone but may have distinct roles within each of these compartments and different aging-induced impacts in their behaviors. There was a smaller age-related decline in the percentage of osteocytes engaged in LCS bone mineralization in cancellous versus cortical bone (-31% vs -58%, **Figure 3**). While the dynamics of bone turnover did not change significantly with age in cortical bone (i.e., comparable rate of decrease in labeled lacunae from 2d to 16d between ages), age greatly increased the frequency of bone turnover in cancellous bone (**Figure 4**). These data suggest that more osteocytes remain active in cancellous bone and may increase their rate of bone turnover compared with cortical bone. Cancellous bone is known to be more metabolically active than cortical bone<sup>29–31</sup>. It is possible that cancellous osteocytes have increased burden of participating in calcium homeostasis in the aging skeleton, but this hypothesis remains speculative at this time.

Our data suggest that the smaller lacunae reported in numerous imaging studies of the aging skeleton<sup>11–16</sup> are associated with decreased osteocyte bone turnover. From coupling scanning electron microscopy measurements of lacunae with fluorochrome labeling, we find that osteocytes that are engaged in recent bone mineralization, regardless of the age group, reside within larger lacunae compared to osteocytes without labels (**Figure 7**). This result suggests that bone resorption events remove a considerable quantity of bone. It is yet to be fully determined which specific additional factors osteocytes employ to promote, or inhibit, local bone mineralization and/or formation. For example, it is well established that osteoblasts participate in local bone mineralization through shuttling hydroxyapatite precursors in vesicles to be released near forming surfaces<sup>57</sup>. Whether osteocytes engage in these active mineralization or mineral inhabitation processes should be investigated.

The influence of aging on osteocyte peri-LCS turnover may be associated with tissue strain. As an initial test of this relationship, we assessed changes in peri-LCS turnover with the spatial position of

osteocytes within the cortical femur. We tested the association of peri-LCS turnover activities between the different quadrants of the mouse femoral cross-section, which vary in strain magnitudes and directions, as well as the variation in intercortical tissue strain with distance from the femoral centroid 43 (Figure 6). In young adult mice, we did not find sufficient evidence to support the hypothesis that peri-LCS turnover depends on the position of osteocytes within the femur cortex. However, in early old age mice, we found evidence that osteocyte LCS bone mineralization depends on the position of osteocytes within the cortical femur. Compared with osteocytes in anterior and posterior regions of cortical bone (i.e., higher tensile and compressive strains under loading, respectively <sup>38,39</sup>), more osteocytes in the medial region of aged bones (i.e., closer to neutral axis) were engaged in LCS bone mineralization (i.e., highest percentage of 2d labels) and the peri-LCS turnover rate was decreased (i.e., smallest change in the presence of 16d labels compared to 2d labels). Additionally, for aged mice, there was a stronger relationship between the position of lacunae within the cortical thickness and peri-LCS mineralization, where 2d labels were more abundant in both endocortical and periosteal surfaces compared to the middle section and 16d labels were the most abundant closest to the periosteal surface. These data suggest that there may be an association between intracortical strain and LCS bone turnover activities that is evident in aging. However, there are important limitations to this analysis, as the observed spatial interactions with peri-LCS turnover could be contributed to by factors other than tissue strain, such as specific nutrient gradients, tissue maturity variations, access to biochemical signals, and differences in shear stress induced by interstitial fluid flow between different cortical ROIs and intracortical distances<sup>43,58–61</sup>. Future research needs to determine if and how peri-LCS turnover is associated with changes in skeletal strain, whether there is a minimum strain required to engage osteocyte peri-LCS turnover, and if this strain threshold changes with aging.

496

497

498 499

500

501

502

503504

505

506

507

508

509

510

511

512

513

514515

516

517

518519

520521

522

523524

525

526

527528

529

With aging, osteocytes become less mechanosensitive<sup>7–10,13,17</sup>. A persistent question is why aging has this effect on these long-lived cells. It has been recognized for many years that substantial strain amplification must occur for osteocytes to respond with anabolic signals to normal skeletal loads<sup>32,62,63</sup>. The changes in lacunar and canalicular shape with age may reduce tissue strain and fluid flow shear stress to contribute to these age-related changes in strain experienced by the cell, as shown by several finite element modeling studies <sup>34,64</sup>. Our data add to this understanding by showing that changes in osteocyte lacunar size with age are approximately bimodal in distribution (i.e., only some aged osteocytes have much reduced lacunar size). Further, we show that labeled osteocyte lacunae are larger than non-labeled lacunae at both ages. Lacunar enlargement with recent peri-LCS turnover activity has been previously shown under high calcium demands such as lactation or PTH treatment <sup>19,22,24,65</sup>. Our observations suggest that contributions to osteocyte mechanosensation derived from geometric factors (i.e., shape of lacunae and canaliculi and the impact of these shape changes on fluid flow) is likely influenced by the activity of

these cells in turning over their local bone. Additionally, our prior work demonstrated that labeled osteocyte lacunae are surrounded by more compliant (i.e., lower modulus) bone<sup>26</sup>. Thus, changes to peri-LCS turnover in aging have multiple potential avenues for altering strain experienced by osteocytes. Our result that aging decreases the percentage of osteocytes engaged in LCS bone mineralization and resorption, but not the apparent rate of label disappearance (i.e., an estimate of resorption), may align with data from studies on the impact of aging on calcium signaling. In the cortical bone of 22 mo female C57BL/6JN mice, there are fewer osteocytes (~ -60%) with active calcium signaling compared to younger mice, yet the remaining osteocytes respond to mechanical load with Ca<sup>2+</sup> peaks of comparable intensities to those observed in young mice<sup>7</sup>. It is not yet understood whether populations of aged osteocytes with different LCS bone turnover characteristics vary in their mechanosensitivity. Together, these data suggest that major gaps still exist in our understanding about the strain experienced by the osteocyte and how these strains change in aging.

Our data also add to the emerging understanding of the osteocyte as a cell with the potential to directly modify bone matrix properties. Studies on transgenic mice with suppressed TGF- $\beta$  or YAP/TAZ signaling, or systemic MMP13 deletion, demonstrate that mice with a decreased ability to engage peri-LCS turnover have more fragile cortical bone<sup>17,27,28,66</sup>. A recent study explored the role of osteocytes in the loss of bone matrix quality in aging by distinguishing matrix characteristics that decline in aging in a manner that is either TGF $\beta$ -dependent or -independent. The study demonstrated an essential role for osteocyte TGF $\beta$  signaling in regulating not only LCS integrity but also collagen material behavior. By contrast, mineral characteristics were regulated independently of TGF $\beta$  signaling<sup>17</sup>. We add to this understanding by showing that osteocyte interaction with bone matrix significantly decreases in age. In addition, our earlier work showed that peri-LCS turnover increases perilacunar bone compliance in both young adult (5 mo) and early-old-aged (22 mo) mice<sup>26</sup>. Together, these data build an argument towards the importance of the osteocyte in maintaining bone matrix quality and the decline of these matrix-regulatory processes in aging.

Aging impacts LCS geometry in both humans and rodents, such as decreased lacunar and canalicular size and connectivity<sup>16,67–70</sup>. If aging also reduces LCS turnover in humans in a similar way that is seen for mice in this study, the quality of a large amount of bone tissue could be impacted. An adult human skeleton contains approximately 42 billion osteocytes each with a lacunar surface area of roughly 336 µm², compromising a 215 m² total surface area<sup>71,72</sup>. From AFM²6 and synchrotron microscopy data<sup>69,73,74</sup>, the region of bone tissue impacted by LCS turnover might be estimated to extend to about 1 micrometer from lacunar walls. Assuming a similar reduction from 80% to 50% of osteocytes engaged in LCS turnover in aging for humans, the amount of bone tissue impacted by this bone turnover would decrease from 4.7 m² to 2.4 m². Importantly, these estimates are only based on peri-lacunar bone turnover and not

peri-canalicular bone turnover and are therefore most likely underestimates. Determining peri-LCS turnover dynamics and the impacts of aging in humans is an important future research direction.

There were several important limitations to this study. First, age-related changes in metabolic processes and LCS network architecture may impact fluorochrome dye uptake between cells in young and old bones, and this limitation should be addressed in future studies. However, our work provides key recommendations for measuring the dynamics of LCS bone mineralization. We find that 2d and 4d labels do not yield statistically significant results across different skeletal sites and ages. In contrast, 8d labels show differences from 2d labels in aged cortical bones and both ages for cancellous bone, while 16d labels are consistently lower compared to 2d labels across all groups. We also found that the order of labeling (calcein first, then alizarin, or vice versa) does not affect the results. In this study, we did not investigate the impact of aging on LCS bone resorption, as indicated by MMP14+ lacunae, through other resorption biomarkers such as TRAP, cathepsin K, or MMP13, but this would be valuable in future investigations. Additionally, our study focused solely on female mice, whereas the literature highlights important sex differences in osteocyte physiology<sup>17,75</sup>. Moreover, extending the age range of the study would be beneficial to exploring whether peri-LCS turnover changes during the developmental and advanced ages. In this study, it was not possible to investigate the age of individual osteocytes in older bones and discern whether the active osteocytes were young or old.

In summary, this study presents the first evidence that osteocyte participation in mineralizing their surroundings is highly abundant in both cortical and cancellous bone of young adult female C57BL/6JN mice. In aging, there are fewer osteocytes with active peri-LCS turnover (both bone mineralization and resorption), yet turnover dynamics remain mostly similar in cortical bone of 5 mo and 22 mo mice, suggesting that active osteocytes engage in a characteristic peri-LCS turnover response. Our results also demonstrate that the impacts of aging on peri-LCS turnover are not uniform throughout the femoral cortex and might differ with tissue strain. The large decline in peri-LCS turnover in aging can have significant implications for bone quality, since osteocytes with active turnover have larger lacunae in both age groups as well as more compliant perilacunar tissue<sup>26</sup>. These results together signify a potential role for osteocyte bone turnover in the loss of bone fracture resistance and changes in mechanosensation in aging.

#### Acknowledgments

This research was made possible by the Department of Mechanical & Industrial Engineering and the College of Engineering at the Montana State University. This work represents the views of the authors and not necessarily those of the sponsors. Research reported here is supported by NSF 2120239 and NIH R03AG068680. Imaging method development and data collection were made possible by the help of Dr.

Heidi Smith from the Center for Biofilm Engineering imaging facility at Montana State University, supported by funding from the National Science Foundation MRI Program (2018562), the M. J. Murdock Charitable Trust (202016116), the US Department of Defense (77369LSRIP & W911NF1910288), and by the Montana Nanotechnology Facility (an NNCI member supported by NSF Grant ECCS-2025391). We thank Dr. Albert Parker for his assistance in statistical analyses. Steven Watson is thanked for his help with image processing and dissection. Kenna Brown and Connor Devine are thanked for their assistance with tissue harvest. Grace Roaming, Chloe Woodwall, and Shane Stauffer are thanked for their help with sample preparation. We thank Fatema Aljamal, Leah Davidson, Torie Prall, Megan Brenna, Kelly Silk, and Allison Stevens for their help with initial steps of method development for this project. Alexey Dynkin is appreciated for manuscript proofreading. We thank Montana State University's Animal Resource Center staff and especially Tamara Marcotte for the help in providing excellent mouse care.

#### **Author Contributions**

Ghazal Vahidi: Investigation; methodology; data curation; formal analysis; visualization; writing – original draft; writing – review and editing. Connor Boone: Investigation; methodology; writing – review and editing. Fawn Hoffman: Formal analysis; Investigation; methodology; writing – review and editing. Chelsea Heveran: Conceptualization; methodology; formal analysis; resources; project administration; supervision; writing - original draft; writing - review and editing.

#### **Declarations of interest:** none

- 618 References
- 619 1. Ensrud, K. E. Epidemiology of fracture risk with advancing age. *Journals of Gerontology Series*
- A Biological Sciences and Medical Sciences 68, 1236–1242 (2013). 10.1093/gerona/glt092
- 621 2. Bonewald, L. F. The amazing osteocyte. *Journal of bone and mineral research* **26**, 229–238
- 622 (2011).
- Schaffler, M. B., Cheung, W. Y., Majeska, R. & Kennedy, O. Osteocytes: Master orchestrators of
- 624 bone. Calcif Tissue Int **94**, 5–24 (2014). PMC3947191
- 4. Alliston, T. Biological regulation of bone quality. *Curr Osteoporos Rep* **12**, 366–375 (2014).
- 626 10.1007/s11914-014-0213-4
- 5. Sherk, V. D. & Rosen, J. Senescent and apoptotic osteocytes and aging: Exercise to the rescue?
- 628 **121**, 255–258 (2019). PMC6459182
- 629 6. Jilka, R. L., Noble, B. & Weinstein, R. S. Osteocyte apoptosis. *Bone* **54**, 264–271 (2013).
- 630 PMC3624050
- 631 7. Morrell, A. E., Robinson, S. T., Silva, M. J. & Guo, X. E. Mechanosensitive Ca2+ signaling and
- coordination is diminished in osteocytes of aged mice during ex vivo tibial loading. Connect
- 633 Tissue Res **61**, 389–398 (2020). 10.1080/03008207.2020.1712377
- 8. Hemmatian, H., Bakker, A. D., Klein-Nulend, J. & van Lenthe, G. H. Aging, Osteocytes, and
- Mechanotransduction. Curr Osteoporos Rep 15, 401–411 (2017).
- 636 9. Razi, H. et al. Aging leads to a dysregulation in mechanically driven bone formation and
- 637 resorption. Journal of Bone and Mineral Research 30, 1864–1873 (2015).
- 638 10. Holguin, N., Brodt, M. D., Sanchez, M. E. & Silva, M. J. Aging diminishes lamellar and woven
- bone formation induced by tibial compression in adult C57BL/6. Bone 65, 83–91 (2014).
- 640 10.1016/j.bone.2014.05.006
- 641 11. Heveran, C. M. & Boerckel, J. D. Osteocyte Remodeling of the Lacunar-Canalicular System:
- What's in a Name? Current Osteoporosis Reports **21**, 11–20 (2023). 10.1007/s11914-022-00766-3
- 643 12. Vahidi, G., Rux, C., Sherk, V. D. & Heveran, C. M. Lacunar-canalicular bone remodeling:
- impacts on bone quality and tools for assessment. *Bone* 115663 (2020).
- doi:10.1016/j.bone.2020.115663 10.1016/j.bone.2020.115663
- 646 13. Schurman, C. A., Verbruggen, S. W. & Alliston, T. Disrupted osteocyte connectivity and
- pericellular fluid flow in bone with aging and defective TGF-β signaling. *Proceedings of the*
- National Academy of Sciences 118, e2023999118 (2021). 10.1073/pnas.2023999118/-
- 649 /DCSupplemental
- 650 14. Tiede-Lewis, L. A. M. & Dallas, S. L. Changes in the osteocyte lacunocanalicular network with
- aging. Bone 122, 101–113 (2019). 10.1016/j.bone.2019.01.025

- 15. Tiede-Lewis, L. M. et al. Degeneration of the osteocyte network in the C57Bl/6 mouse model of
- aging. Aging 9, 2190–2208 (2017). PMC5680562
- 16. Heveran, C. M., Rauff, A., King, K. B., Carpenter, R. D. & Ferguson, V. L. A new open-source
- tool for measuring 3D osteocyte lacunar geometries from confocal laser scanning microscopy
- reveals age-related changes to lacunar size and shape in cortical mouse bone. *Bone* **110**, (2018).
- 657 PMC5878731
- 658 17. Schurman, C. A. et al. Aging impairs the osteocytic regulation of collagen integrity and bone
- 659 quality. Bone Res 12, 13 (2024). 10.1038/s41413-023-00303-7
- 660 18. Kaya, S. et al. Lactation-induced changes in the volume of osteocyte lacunar-canalicular space
- alter mechanical properties in cortical bone tissue. *Journal of Bone and Mineral Research* 32,
- 662 688–697 (2017). PMC5395324
- 663 19. Qing, H. et al. Demonstration of osteocytic perilacunar/canalicular remodeling in mice during
- 664 lactation. Journal of Bone and Mineral Research 27, 1018–1029 (2012). 10.1002/jbmr.1567
- 665 20. Lane, N. E. et al. Glucocorticoid-treated mice have localized changes in trabecular bone material
- properties and osteocyte lacunar size that are not observed in placebo-treated or estrogen-deficient
- mice. Journal of Bone and Mineral Research 21, 466–476 (2006). 10.1359/JBMR.051103
- 668 21. Gardinier, J. D., Al-Omaishi, S., Morris, M. D. & Kohn, D. H. PTH signaling mediates perilacunar
- remodeling during exercise. *Matrix Biology* **52–54**, 162–175 (2016). PMC4875803
- 570 22. Jähn, K. et al. Osteocytes Acidify Their Microenvironment in Response to PTHrP In Vitro and in
- 671 Lactating Mice In Vivo. *Journal of Bone and Mineral Research* **32**, 1761–1772 (2017).
- 672 10.1002/jbmr.3167
- 673 23. Yajima, A. et al. Osteocytic perilacunar/canalicular turnover in hemodialysis patients with high
- and low serum PTH levels. *Bone* **113**, 68–76 (2018). 10.1016/j.bone.2018.05.002
- 675 24. Qing, H. & Bonewald, L. F. Osteocyte remodeling of the perilacunar and pericanalicular matrix.
- 676 International journal of oral science 1, 59–65 (2009). 10.4248/ijos.09019
- 677 25. Tazawa, K. et al. Osteocytic osteolysis observed in rats to which parathyroid hormone was
- 678 continuously administered. *J Bone Miner Metab* **22**, 524–529 (2004). 10.1007/s00774-004-0519-x
- 679 26. Rux, C. J., Vahidi, G., Darabi, A., Cox, L. M. & Heveran, C. M. Perilacunar bone tissue exhibits
- sub-micrometer modulus gradation which depends on the recency of osteocyte bone formation in
- both young adult and early-old-age female C57Bl/6 mice. *Bone* 157, (2022).
- 682 10.1016/j.bone.2022.116327
- 683 27. Tang, S., Herber, R.-P., Ho, S. & Alliston, T. Matrix Metalloproteinase-13 is Required for
- 684 Osteocytic Perilacunar Remodeling and Maintains Bone Fracture Resistance SY. *J Bone Miner*
- 685 Res. 27, 1936–1950 (2012). 10.1002/jbmr.1646.Matrix

- 686 28. Kegelman, C. D. et al. YAP and TAZ Mediate Osteocyte Perilacunar/Canalicular Remodeling.
- *Journal of Bone and Mineral Research* **00**, 1–15 (2019). 10.1002/jbmr.3876
- 688 29. Hadjidakis, D. J. & Androulakis, I. I. Bone remodeling. *Ann N Y Acad Sci* **1092**, 385–396 (2006).
- 689 30. Delmas, P. D. Biochemical markers of bone turnover for the clinical assessment of metabolic bone
- disease. Endocrinol Metab Clin North Am 19, 1–18 (1990).
- 691 31. Shahnazari, M. et al. Bone turnover markers in peripheral blood and marrow plasma reflect
- trabecular bone loss but not endocortical expansion in aging mice. *Bone* **50**, 628–637 (2012).
- 693 10.1016/j.bone.2011.11.010
- 694 32. Wang, Y., Mcnamara, L. M., Schaffler, M. B. & Weinbaum, S. Strain amplification and integrin
- *based signaling in osteocytes.*
- 696 33. Lewis, K. J. et al. Estrogen depletion on In vivo osteocyte calcium signaling responses to
- mechanical loading. *Bone* **152**, (2021). 10.1016/j.bone.2021.116072
- 698 34. Nazer, R. Al, Lanovaz, J., Kawalilak, C., Johnston, J. D. & Kontulainen, S. Direct in vivo strain
- measurements in human bone A systematic literature review. *J Biomech* **45**, 27–40 (2012).
- 700 10.1016/j.jbiomech.2011.08.004
- 701 35. Nicolella, D. P. et al. Effects of nanomechanical bone tissue properties on bone tissue strain:
- 702 Implications for osteocyte mechanotransduction. *Journal of Musculoskeletal Neuronal*
- 703 *Interactions* **8**, 330–331 (2008).
- 704 36. Lai, X., Chung, R., Li, Y., Liu, X. S. & Wang, L. Lactation alters fluid flow and solute transport in
- 705 maternal skeleton: A multiscale modeling study on the effects of microstructural changes and
- 706 loading frequency. *Bone* **151**, (2021). 10.1016/j.bone.2021.116033
- 707 37. Sang, W. & Ural, A. Quantifying how altered lacunar morphology and perilacunar tissue
- 708 properties influence local mechanical environment of osteocyte lacunae using finite element
- 709 modeling. *J Mech Behav Biomed Mater* **135**, (2022). 10.1016/j.jmbbm.2022.105433
- 710 38. Rudman, K. E., Aspden, R. M. & Meakin, J. R. Compression or tension? The stress distribution in
- 711 the proximal femur. *Biomed Eng Online* **5**, (2006). 10.1186/1475-925X-5-12
- 712 39. Ramasamy, J. G. & Akkus, O. Local variations in the micromechanical properties of mouse femur:
- The involvement of collagen fiber orientation and mineralization. *J Biomech* **40**, 910–918 (2007).
- 714 10.1016/j.jbiomech.2006.03.002
- 715 40. Bach-Gansmo, F. L. et al. Osteocyte lacunar properties in rat cortical bone: Differences between
- 716 lamellar and central bone. *J Struct Biol* **191**, 59–67 (2015).
- 717 https://doi.org/10.1016/j.jsb.2015.05.005

- 718 41. Palumbo, C. & Ferretti, M. Histomorphometric study on the osteocyte lacuno-canalicular network
- 719 in animals of different species. I. Woven-fibered and parallel-fibered bones. Article in Italian
- *Journal of Anatomy and Embryology* (1998).
- 721 42. Schneider, C. A., Rasband, W. S. & Eliceiri, K. W. NIH Image to ImageJ: 25 years of Image
- 722 Analysis HHS Public Access. Nat Methods 9, (2012).
- 723 43. Ascenzi, M. G. et al. Hyperlipidemia affects multiscale structure and strength of murine femur. J
- 724 Biomech 47, 2436–2443 (2014). 10.1016/j.jbiomech.2014.04.006
- 725 44. Poundarik, A. A. & Vashishth, D. Multiscale imaging of bone microdamage. *Connect Tissue Res*
- **56**, 87–98 (2015). 10.3109/03008207.2015.1008133
- 727 45. Burr, D. B. & Hooser, M. Alterations to the En Bloc Basic Fuchsin Staining Protocol for the
- 728 Demonstration of Microdamage Produced In Vivo. Bone 17, (1995).
- 729 46. Hilton, M. J. Skeletal Development and Repair. (Springer, 2016).
- 730 47. Vahidi, G. et al. Germ-Free C57BL/6 Mice Have Increased Bone Mass and Altered Matrix
- Properties but Not Decreased Bone Fracture Resistance. *Journal of Bone and Mineral Research*
- 732 **38**, 1154–1174 (2023). 10.1002/jbmr.4835
- 733 48. Milovanovic, P. & Busse, B. Inter-site variability of the human osteocyte lacunar network:
- implications for bone quality. *Curr Osteoporos Rep* **17**, 105–115 (2019).
- 735 49. Ashique, A. M. et al. Lacunar-canalicular network in femoral cortical bone is reduced in aged
- women and is predominantly due to a loss of canalicular porosity. *Bone Rep* 7, 9–16 (2017).
- 737 10.1016/j.bonr.2017.06.002
- 738 50. Paschalis, E. P. et al. Aging Versus Postmenopausal Osteoporosis: Bone Composition and
- 739 Maturation Kinetics at Actively-Forming Trabecular Surfaces of Female Subjects Aged 1 to 84
- 740 Years. Journal of Bone and Mineral Research 31, 347–357 (2016). 10.1002/jbmr.2696
- Horr, D. B. Changes in bone matrix properties with aging. *Bone* **120**, 85–93 (2019).
- 742 10.1016/j.bone.2018.10.010
- 743 52. Creecy, A. et al. The age-related decrease in material properties of BALB/c mouse long bones
- involves alterations to the extracellular matrix. *Bone* **130**, 115126 (2020).
- 745 10.1016/j.bone.2019.115126
- 746 53. Cui, J., Shibata, Y., Zhu, T., Zhou, J. & Zhang, J. Osteocytes in bone aging: Advances, challenges,
- and future perspectives. Ageing Research Reviews 77, (2022). 10.1016/j.arr.2022.101608
- 748 54. Ferretti, M., Muglia, M. A., Remaggi, F., Cane, V. & Palumbo, C. Histomorphometric study on
- 749 the osteocyte lacuno-canalicular network in animals of different species. II. Parallel-fibered and
- 750 lamellar bones. *Ital J Anat Embryol* **104**, 121–131 (1999).

- 751 55. Schemenz, V. et al. Heterogeneity of the osteocyte lacuno-canalicular network architecture and
- material characteristics across different tissue types in healing bone. *J Struct Biol* **212**, (2020).
- 753 10.1016/j.jsb.2020.107616
- 754 56. Hernandez, C. J., Majeska, R. J. & Schaffler, M. B. Osteocyte density in woven bone. *Bone* 35,
- 755 1095–1099 (2004). 10.1016/j.bone.2004.07.002
- 756 57. Hasegawa, T. Ultrastructure and biological function of matrix vesicles in bone mineralization.
- 757 *Histochemistry and Cell Biology* **149**, 289–304 (2018). 10.1007/s00418-018-1646-0
- 758 58. Golan, S., Elata, D. & Dinnar, U. Cortical Bone Periosteocytic Space Morphology Can Affect
- Osteocyte-Level Mass Flows and Shear Stresses. in Engineering Systems Design and Analysis
- 760 **48364**, 77–84 (2008).
- 761 59. Rohrbach, D. et al. Spatial distribution of tissue level properties in a human femoral cortical bone.
- 762 *J Biomech* **45**, 2264–2270 (2012). 10.1016/j.jbiomech.2012.06.003
- 763 60. Birkhold, A. I., Razi, H., Duda, G. N., Checa, S. & Willie, B. M. Tomography-Based
- Quantification of Regional Differences in Cortical Bone Surface Remodeling and Mechano-
- 765 Response. Calcif Tissue Int **100**, 255–270 (2017). 10.1007/s00223-016-0217-4
- 766 61. Sun, Y. et al. Mechanical Stimulation on Mesenchymal Stem Cells and Surrounding
- 767 Microenvironments in Bone Regeneration: Regulations and Applications. Frontiers in Cell and
- 768 Developmental Biology 10, (2022). 10.3389/fcell.2022.808303
- 769 62. Han, Y., Cowin, S. C., Schaffler, M. B. & Weinbaum, S. Mechanotransduction and strain
- amplification in osteocyte cell processes. PNAS 101, (2004).
- 771 63. Rath Bonivtch, A., Bonewald, L. F. & Nicolella, D. P. Tissue strain amplification at the osteocyte
- 772 lacuna: A microstructural finite element analysis. *J Biomech* **40**, 2199–2206 (2007).
- 773 10.1016/j.jbiomech.2006.10.040
- 774 64. McCreadie, B. R., Hollister, S. J., Schaffler, M. B. & Goldstein, S. A. Osteocyte lacuna size and
- shape in women with and without osteoporotic fracture. *J Biomech* **37**, 563–572 (2004).
- 776 10.1016/S0021-9290(03)00287-2
- 777 65. Belanger, L. R. Osteocytic Osteolysis. *Calcif Tissue Int* **12**, 1–12 (1969).
- 778 66. Dole, N. S. *et al.* Osteocyte-intrinsic TGF-β signaling regulates bone quality through
- perilacunar/canalicular remodeling. *Cell Rep* **21**, 2585–2596 (2017).
- 780 67. Schurman, C. A., Verbruggen, S. W. & Alliston, T. Disrupted osteocyte connectivity and
- pericellular fluid flow in bone with aging and defective TGF- β signaling. 1–11 (2021).
- 782 doi:10.1073/pnas.2023999118/-/DCSupplemental.Published 10.1073/pnas.2023999118/-
- 783 /DCSupplemental.Published

- 784 68. Carter, Y., Thomas, C. D. L., Clement, J. G. & Cooper, D. M. L. Femoral osteocyte lacunar
- density, volume and morphology in women across the lifespan. *J Struct Biol* **183**, 519–526 (2013).
- 786 10.1016/j.jsb.2013.07.004
- 787 69. Carter, Y. et al. Variation in osteocyte lacunar morphology and density in the human femur—a
- 788 synchrotron radiation micro-CT study. *Bone* **52**, 126–132 (2013).
- 789 70. Bach-Gansmo, F. L. et al. Osteocyte lacunar properties and cortical microstructure in human iliac
- 790 crest as a function of age and sex. *Bone* **91**, 11–19 (2016).
- 791 71. Buenzli, P. R. & Sims, N. A. Quantifying the osteocyte network in the human skeleton. *Bone* 75,
- 792 144–150 (2015). 10.1016/j.bone.2015.02.016
- 793 72. Dong, P. et al. 3D osteocyte lacunar morphometric properties and distributions in human femoral
- 794 cortical bone using synchrotron radiation micro-CT images. *Bone* **60**, 172–185 (2014).
- 795 10.1016/j.bone.2013.12.008
- 73. Varga, P. et al. Investigation of the three-dimensional orientation of mineralized collagen fibrils in
- human lamellar bone using synchrotron X-ray phase nano-tomography. Acta Biomater 9, 8118–
- 798 8127 (2013). 10.1016/j.actbio.2013.05.015
- 799 74. Hesse, B. et al. Canalicular network morphology is the major determinant of the spatial
- distribution of mass density in human bone tissue: Evidence by means of synchrotron radiation
- phase-contrast nano-CT. *Journal of Bone and Mineral Research* **30**, 346–356 (2015).
- 802 10.1002/jbmr.2324

806

- 803 75. Matthews, M. M., Cook, E., Naguib, N., Wiesner, U. B. & Lewis, K. J. Intravital imaging of
- osteocyte integrin dynamics with locally injectable fluorescent nanoparticles. *Bone* **174**, (2023).
- 805 10.1016/j.bone.2023.116830